Experimental Eye Research 238 (2024) 109727

Contents lists available at ScienceDirect

Experimental Eye Research

journal homepage: www.elsevier.com/locate/yexer

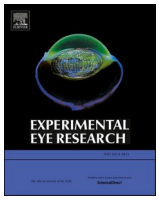

Research article

High-fat diet causes endothelial dysfunction in the mouse ophthalmic artery

Subao Jiang [a,*], Ning Xia [b], Francesco Buonfiglio [a], Elsa W. Böhm [a], Qi Tang [a], Norbert Pfeiffer [a], Dominik Olinger [b], Huige Li [b], Adrian Gericke [a]

[a] Department of Ophthalmology, University Medical Center, Johannes Gutenberg University Mainz, Langenbeckstrasse 1, 55131, Mainz, Germany
[b] Department of Pharmacology, University Medical Center, Johannes Gutenberg University Mainz, Langenbeckstrasse 1, 55131, Mainz, Germany

ARTICLE INFO

Keywords:
Endothelial dysfunction
High-fat diet (HFD)
Ophthalmic artery (OA)
Receptor for advanced glycation end products (RAGE)
Lectin-like oxidized low-density-lipoprotein receptor-1 (LOX-1)

ABSTRACT

Obesity is a significant health concern that leads to impaired vascular function and subsequent abnormalities in various organs. The impact of obesity on ocular blood vessels, however, remains largely unclear. In this study, we examined the hypothesis that obesity induced by high-fat diet produces vascular endothelial dysfunction in the ophthalmic artery. Mice were subjected to a high-fat diet for 20 weeks, while age-matched controls were maintained on a standard diet. Reactivity of isolated ophthalmic artery segments was assessed in vitro. Reactive oxygen species (ROS) were quantified in cryosections by dihydroethidium (DHE) staining. Redox gene expression was determined in ophthalmic artery explants by real-time PCR. Furthermore, the expression of nicotinamide adenine dinucleotide phosphate oxidase 2 (NOX2), the receptor for advanced glycation end products (RAGE), and of the lectin-like oxidized low-density-lipoprotein receptor-1 (LOX-1) was determined in cryosections using immunofluorescence microscopy. Ophthalmic artery segments from mice on a high-fat diet exhibited impaired vasodilation responses to the endothelium-dependent vasodilator acetylcholine, while endothelium-independent responses to nitroprusside remained preserved. DHE staining intensity in the vascular wall was notably stronger in mice on a high-fat diet. Messenger RNA expression for NOX2 was elevated in the ophthalmic artery of mice subjected to high fat diet. Likewise, immunostainings revealed increased expression of NOX2 and of RAGE, but not of LOX-1. These findings suggest that a high-fat diet triggers endothelial dysfunction by inducing oxidative stress in the ophthalmic artery via involvement of RAGE and NOX2.

1. Introduction

Obesity is a pathological condition characterized by a body mass index (BMI) of 30 kg/m^2 or higher, calculated by dividing weight in kilograms by height in square meters (Apovian, 2016). It poses a growing challenge to public health worldwide and is associated with severe comorbidities such as hyperlipidemia, diabetes mellitus, arterial hypertension, atherosclerosis, and an increased risk for developing metabolic syndrome, a cluster of conditions associated with higher morbidity and mortality (Bray, 2004; Mozaffarian et al., 2011; Li et al., 2020). High-fat diet (HFD) is commonly used as an experimental animal model to study diet-induced obesity, which is characterized by a caloric intake ranging from 30% to 75% from fat (Li et al., 2020). Previous studies have strongly linked a high-fat diet to heart disease, cancer, and other chronic degenerative diseases (Health, I. of M. C. on D. et al., 1992). Given the strong association between HFD, obesity, hypercholesterolemia, insulin resistance, and diabetes, mice fed a high-fat diet are often considered a model for these conditions (Nagy and Einwallner, 2018; Wang and Liao, 2012a; Zhang et al., 2020). Of note, previous studies have demonstrated that hyperlipidemia can lead to altered retinal function (Chang et al., 2015; Kopec et al., 2017; Zhang et al., 2014). For example, both scotopic and photopic electroretinogram (ERG) responses were shown to be reduced in mice on a HFD (Chang et al., 2015). Obesity contributes to chronic low-grade inflammation and promotes a prothrombotic state (Allende-Vigo, 2010; Ouchi et al., 2011). Increased thrombin activity associated with excess fat can trigger thromboembolic events, posing a risk for retinal embolism, a condition that can significantly impact vision. Despite significant progress in

* Corresponding author.
E-mail addresses: sjiang@uni-mainz.de (S. Jiang), xianing@uni-mainz.de (N. Xia), fbuonfig@uni-mainz.de (F. Buonfiglio), ElsaWilma.Boehm@unimedizin-mainz.de (E.W. Böhm), qitang.med@gmail.com (Q. Tang), norbert.pfeiffer@unimedizin-mainz.de (N. Pfeiffer), dominikolinger@gmail.com (D. Olinger), huigeli@uni-mainz.de (H. Li), adrian.gericke@unimedizin-mainz.de (A. Gericke).

https://doi.org/10.1016/j.exer.2023.109727
Received 13 July 2023; Received in revised form 27 October 2023; Accepted 13 November 2023
Available online 14 November 2023

researching the effects of a high-fat diet on blood vessels, there remains a lack of knowledge regarding its impact on ocular vascular function. Given the high prevalence of diet-related diseases, which are expected to continue increasing, it is imperative to gain a comprehensive understanding of the mechanisms and impacts of these conditions while exploring novel treatment opportunities. The primary goal of this research is to investigate the hypothesis that a high-fat diet leads to endothelial dysfunction in the ophthalmic artery of mice. Additionally, this study seeks to elucidate the potential underlying mechanisms associated with this phenomenon.

2. Materials and methods

2.1. Animals

The study adhered to the guidelines set forth in the EU Directive 2010/63EU for animal experiments, and the responsible regulatory authority (Landesuntersuchungsamt Rheinland-Pfalz), approved the protocols involving mice (23 177-07/G 17-1-020). C57BL/6J mice, at the age of 8 weeks, were divided into two groups for the duration of the study. The high-fat diet (HFD) group was provided with a diet containing 45% energy from fat (ssniff Spezialdiäten GmbH, Soest, Germany), while the control group, referred to as the normal-calorie diet (NCD) group, received a standard diet containing 11% energy from fat. HFD-induced obesity is a well-established model. For the development of a full picture of obesity, a HFD feeding time range of >16 weeks is required *(Wang and Liao, 2012b)*. For that reason, we chose an exposure time to either HFD or NCD of 20 weeks as in a previous publication of our own *(Xia* et al., *2016a)*. Both groups were housed under standardized conditions, including 12-h light/dark cycles, a temperature of 22 ± 2 °C, a humidity of 55 ± 10%, and unrestricted access to food and tap water.

2.2. Measurement of body weight and serum parameters

Mice were weighed at the day of experiment. Subsequently, the mice were euthanized by carbon dioxide exposure. Blood samples were collected from the heart, and serum parameters were determined using the scil Reflovet® Plus (scil animal care company GmbH, Viernheim, Germany), following the established protocol *(Zadeh* et al., *2019b)*.

2.3. Measurement of vascular responses

After euthanizing the mice by carbon dioxide inhalation, the eyes were carefully excised and placed in ice-cold Krebs–Henseleit buffer. Segments of the ophthalmic artery were then prepared for functional testing using videomicroscopy, following a previously reported method (Gericke et al., 2009, 2011). Vascular reactivity was assessed after an equilibration period of 45 min. First, concentration-dependent responses to the thromboxane A2 (TP) receptor agonist, U46619 (10^{-11} M to 10^{-6} M; Cayman Chemical, Ann Arbor, MI, USA) were measured. Subsequently, the vessels were pre-constricted with U46619 to achieve a constriction of 50–70% of the initial luminal diameter and concentration-dependent responses to sodium nitroprusside (SNP, 10^{-9} M to 10^{-4} M, Sigma-Aldrich), an endothelium-independent vasodilator, and to acetylcholine (10^{-9} to 10^{-4} M; Sigma-Aldrich, Taufkirchen, Germany), an endothelium-dependent vasodilator in mouse ophthalmic arteries, were then evaluated (Gericke et al., 2014; Manicam et al., 2016).

2.4. Quantification of reactive oxygen species

To quantify the formation of reactive oxygen species (ROS), ophthalmic artery cryosections of 10 μm thickness were treated with dihydroethidium (DHE) at a concentration of 1 μM. The sections were incubated at 37 °C for 30 min. Fluorescence measurements were performed using excitation/emission wavelengths of 518 nm/605 nm. The quantification of ROS formation was conducted in cross-sections of blood vessels following the methodology described in previous studies *(Chronopoulos* et al., *2023)*.

2.5. Quantitative PCR

Following euthanasia via carbon dioxide inhalation, ophthalmic arteries were carefully dissected under a microscope and placed into 1.5 ml plastic tubes, rapidly frozen in liquid nitrogen, and stored at −80 °C for further analysis. For quantitative PCR analysis of mRNA expression for the prooxidant redox enzymes, nicotinamide adenine dinucleotide phosphate oxidase 1, 2, and 4 (NOX1, NOX2, NOX4), and for xanthine dehydrogenase (XDH), the tissue samples were homogenized using the FastPrep system (MP Biomedicals, Illkirch, France). XDH is active primarily as a dehydrogenase under physiological conditions. However, various stimuli, e.g., inflammation and hypoxia, foster the conversion of XDH to the superoxide-producing xanthine oxidase (XO), which triggers endothelial dysfunction and atherosclerosis (Schröder et al., 2006).

Therefore, we use the abbreviation XDH/XO in the publication. The expression of genes was detected using SYBR Green-based quantitative real-time PCR, following the protocol described in previous studies *(Xia* et al., *2016b)*. RNA isolation was performed using peqGOLD TriFast™ (PEQLAB), and cDNA was synthesized using the High Capacity cDNA Reverse Transcription Kit (Applied Biosystems, Darmstadt, Germany). Real-time PCR reactions were carried out on a StepOnePlus™ Real-Time PCR System (Applied Biosystems) using SYBR® Green JumpStart™ Taq ReadyMix™ (Sigma-Aldrich) and 20 ng cDNA. The relative mRNA levels of the target genes were quantified by comparing the threshold cycle (CT) values and normalizing to the housekeeping gene TATA-binding protein (TBP). The messenger RNA expression is presented as the fold-change in mice subjected to HFD compared to mice subjected to normal-calorie diet (NCD). The primer sequences used for PCR are listed in Table 1.

2.6. Immunostainings and histology

To quantify the prooxidatnt enzyme, NOX2, as well as the lectin-like oxidized low-density-lipoprotein receptor-1 (LOX-1) and the receptor for advanced glycation end products (RAGE) on the protein level, we conducted immunofluorescence stainings using specific antibodies in frozen sections. First, the tissue was fixed with 4% paraformaldehyde for 20 min, followed by a wash in phosphate-buffered solution (PBS) for 20 min. Subsequently, the tissue was blocked with 1% fetal bovine serum for 30 min to reduce non-specific binding. The primary antibody was then applied and incubated at room temperature for 2 h. After incubation, the tissue was washed three times with PBS for 5 min each. Next, the appropriate secondary antibody was applied and incubated at room temperature for 2 h to visualize the specific protein targets. Some sections were incubated with blocking medium and the secondary antibody only, omitting the primary antibody, to check for unspecific binding. Following the incubation and washing steps, a DAPI-containing solution (BIOZOL Diagnostica Vertrieb GmbH, Eching, Germany) was applied to each slide to stain the cell nuclei. The slides were then cover-slipped and subjected to fluorescence microscopy for visualization. The specification of the applied antibodies are listed in Table 2. For histology, the cryosections were fixed in formaldehyde for 1 min and rinsed with water for 10 s. Next, sections were immersed in hematoxylin solution for 3 min and washed in purified water for 5 min. Subsequently, the slides were placed for 1 min into 95% ethanol and were stained for 1 min in eosin solution. The slides were then dehydrated in an ascending ethanol series (70, 96, and 100%) following by a bath for 10 min in xylene. Finally, the glass slides were mounted with Eukitt quick-hardening mounting medium (Sigma-Aldrich Chemie, Munich, Germany).

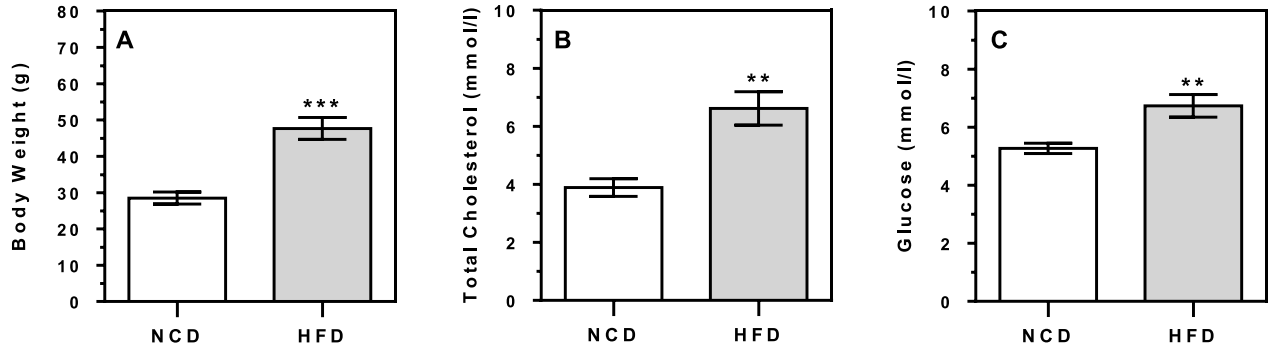

Fig. 1. Body weight (A), serum levels of total cholesterol (B) and of glucose (C) were markedly increased in mice subjected to a high-fat diet (HFD) over a duration of 20 weeks compared to contrals that received a normal chow diet (NCD). Values are expressed as mean ± SE (n = 6 per group; **p < 0.01; ***p < 0.001; HFD versus NCD).

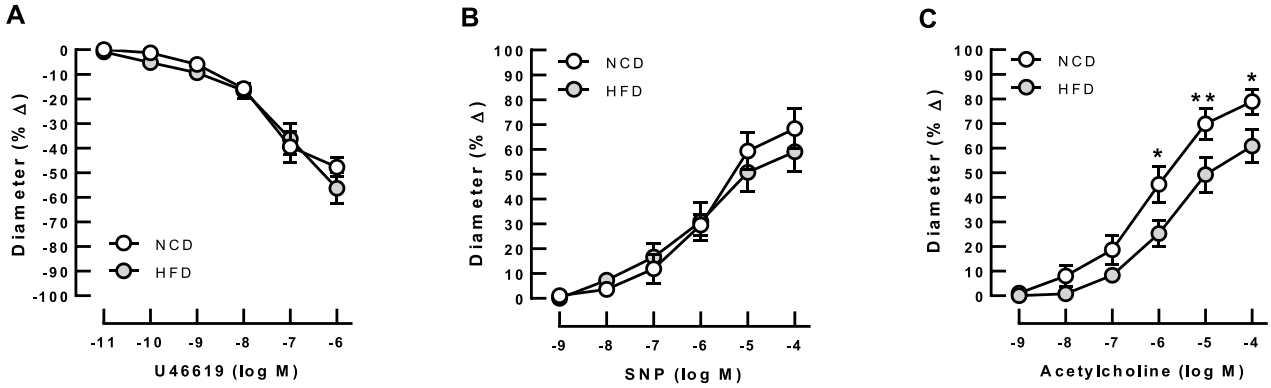

Fig. 2. Exposure to a high-fat diet (HFD) over a duration of 20 weeks did not affect the response of ophthalmic arteries to the vasoconstrictor, U46619 (A), or to the endothelium-independent vasodilator, SNP (B), whereas it did reduce dilation to the endothelium-dependent agonist, acetylcholine (C), compared to responses of arteries from mice that received a normal chow diet (NCD). Values are expressed as mean ± SE (n = 6 per group; *p < 0.05; **p < 0.01; HFD versus NCD).

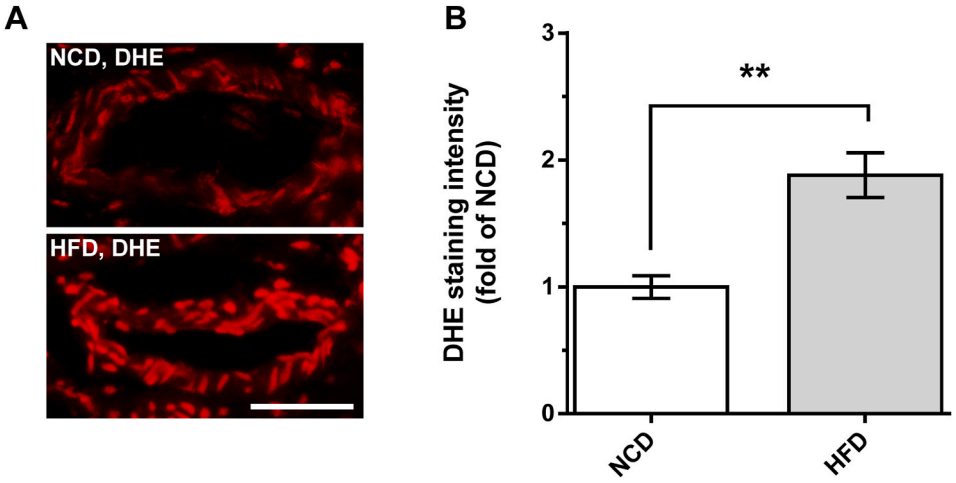

Fig. 3. Ophthalmic artery cross-sections from mice exposed to a high-fat diet (HFD) had a higher fluorescent intensity to dihydroethidium (DHE) than cross-sections from mice on normal chow diet (NCD), suggestive of elevated ROS levels in arteries from mice exposed to HFD. (A and B). Data are expressed as means ± SE (n = 6 per group; **p = 0.0013). Scale bar = 50 μm.

2.7. Statistical analysis

The data is presented as the mean ± standard error (SE), and the value of n represents the number of mice in each group. Statistical analysis was performed using the unpaired t-test to compare serum parameters, fluorescent intensity, and mRNA expression levels between the groups. Contractile responses to U46619 are expressed as a percentage change in luminal diameter relative to the initial resting

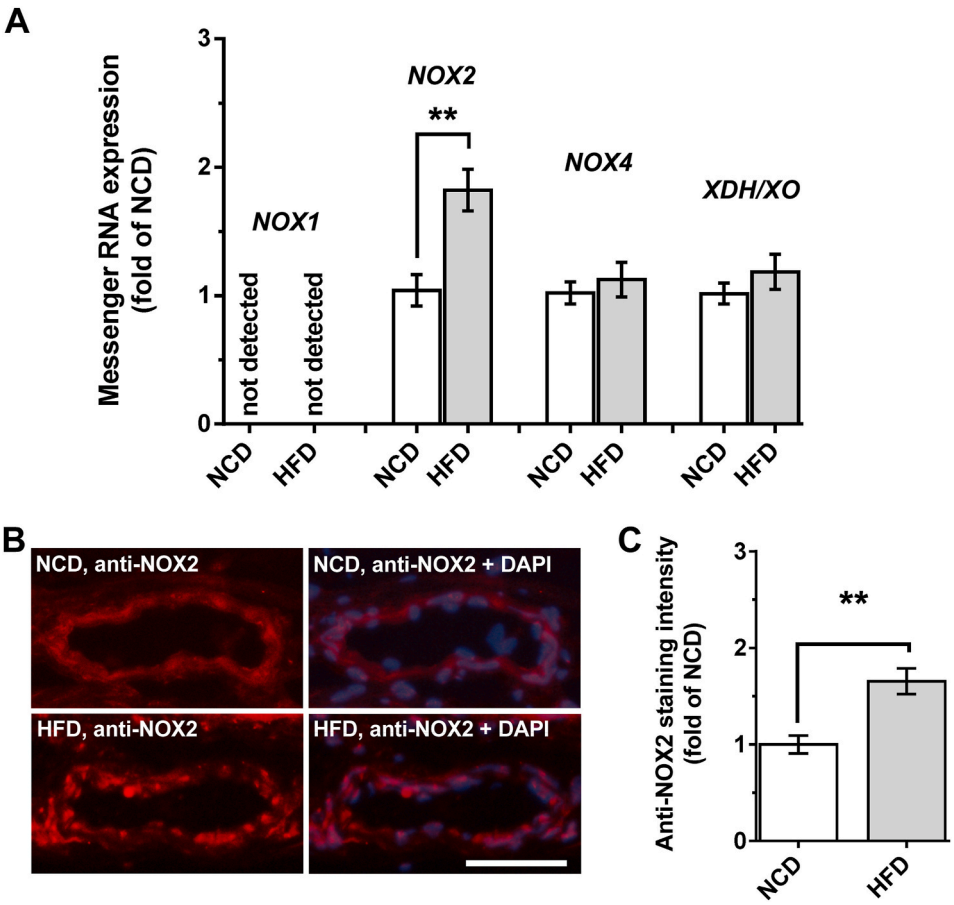

Fig. 4. (A) Messenger RNA (mRNA) expression for several prooxidant enzymes was quantified in ophthalmic artery explants. Whereas no mRNA was detected for NOX1, expression of NOX4 and XDH/XO mRNA was similar in ophthalmic arteries from mice exposed to high fat diet (HFD) and normal chow diet (NCD). Remarkably, expression of mRNA for NOX2 was markedly elevated in ophthalmic arteries from mice on HFD (**p = 0.0033). (B) To quantify NOX2 on the protein level, immunostainings in ophthalmic artery cross-sections were conducted, as shown on representative microphotographs. (C) Immunoreactivity to NOX2 was much stronger in ophthalmic artery cross-sections from mice subjected to HFD compared to mice on NCD (**p = 0.0023). Data are expressed as means ± SE. Scale bar = 50 μm.

diameter. Responses to SNP and acetylcholine are expressed as a percentage change in lumen diameter relative to the diameter after precontraction. Concentration response curves were compared by two-way ANOVA for repeated measurements and a Bonferroni posthoc test. A significance level of 0.05 was chosen to determine statistical significance.

3. Results

3.1. Metabolic parameters

Body weight was remarkably higher in mice exposed to HFD compared to NCD (47.7 ± 3.02 vs. 28.5 ± 1.65; ***p = 0.0002; Fig. 1A), which is a feature of obesity. Likewise, serum levels of total cholesterol were higher in mice subjected to HFD than in mice on NCD (6.62 ± 0.572 vs. 3.89 ± 0.302, **p = 0.0018; Fig. 1B). Serum glucose levels were also markedly elevated in HFD mice (6.73 ± 0.389 vs. 5.27 ± 0.176, **p = 0.0065; Fig. 1C), indicative of diet-induced diabetes.

3.2. Ophthalmic artery responses to vasoactive substances

The thromboxane A2 (TP) receptor agonist, U46619 (10^{-11} M–10^{-6} M), elicited concentration-dependent vasoconstriction that did not differ between ophthalmic arteries from mice subjected to HFD and to NCD (Fig. 2A). There were also no differences between both mouse groups in response to SNP (Fig. 2B). In contrast, responses to the endothelium-dependent vasodilator, acetylcholine, were moderately but significantly reduced in mice subjected to HFD, indicative of endothelial dysfunction (Fig. 2C).

3.3. Levels of reactive oxygen species

DHE staining was used to quantify ROS. DHE is converted by ROS to highly fluorescent oxidized products (e.g., 2-hydroxyethidium, which is specific for superoxide as well as ethidium, which is the unspecific oxidation product formed by hydroxyl radicals via Fenton reaction or peroxide/peroxidase reactivity). Both oxidized DHE products intercalate with the DNA to form highly fluorescent complexes that represent a general read-out of oxidative stress. Of note, DHE fluorescence intensity was markedly elevated in the ophthalmic artery wall of the HFD group compared to the NCD group (Fig. 3).

3.4. Prooxidant redox enzymes in the ophthalmic artery

Notably, mRNA for NOX1 was neither detected in ophthalmic arteries from mice subjected to HFD nor in those exposed to NCD (Fig. 4A). In contrast, NOX2 mRNA expression was markedly elevated in mice exposed to HFD (Fig. 4A). No differences in mRNA expression between both mouse groups were found for NOX4 and for XDH/XO (Fig. 4A). To quantify NOX2 expression on the protein level, immunostainings were performed. In Fig. 4B, representative photomicrographs are presented for ophthalmic artery cross-sections of mice exposed to HFD and NCD.

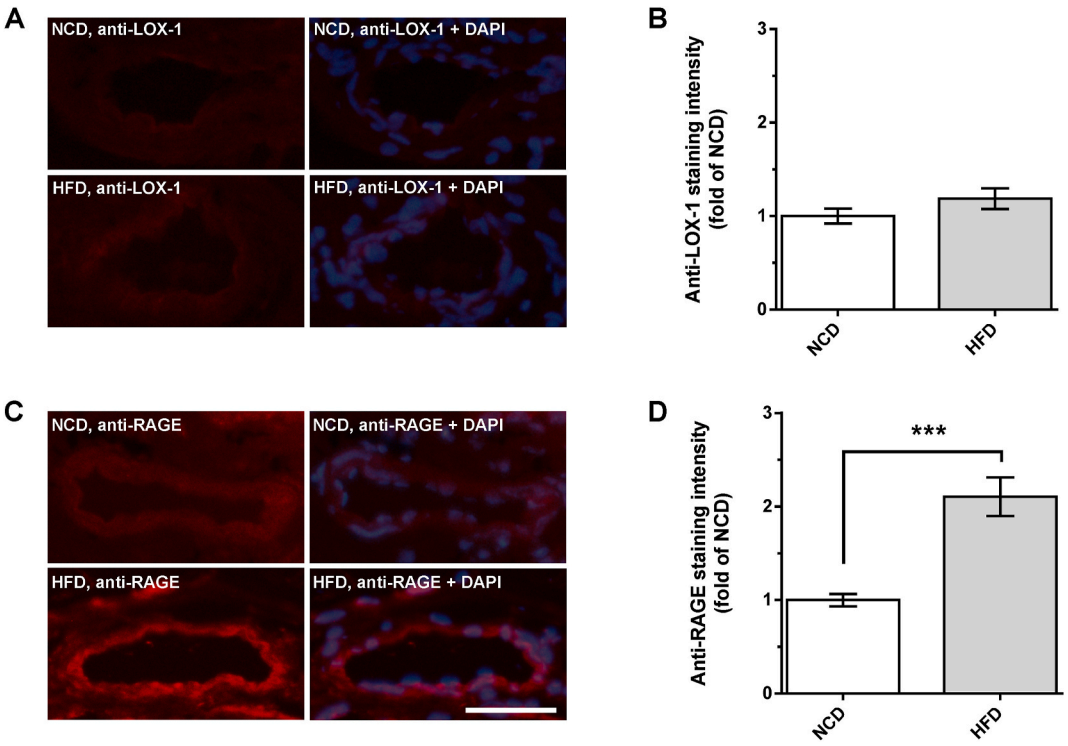

Fig. 5. Quantification of LOX1 and RAGE expression. (A) Anti-LOX-1 receptor immunoreactivity was very faint in both ophthalmic arteries from mice subjected to high fat diet (HFD) and to normal chow diet (NCD). (B) Anti-LOX-1 expression levels did not differ between the HFD and the NCD group. (C) While anti-RAGE immunoreactivity was very weak in ophthalmic artery cross-sections of the NCD group, it was pronounced in the HFD group. (D) Immunoreactivity to RAGE was much stronger in ophthalmic artery cross-sections from mice subjected to HFD compared to mice on NCD. Data are expressed as means ± SE (n = 6 per group; ***p < 0.0005). Scale bar = 50 μm.

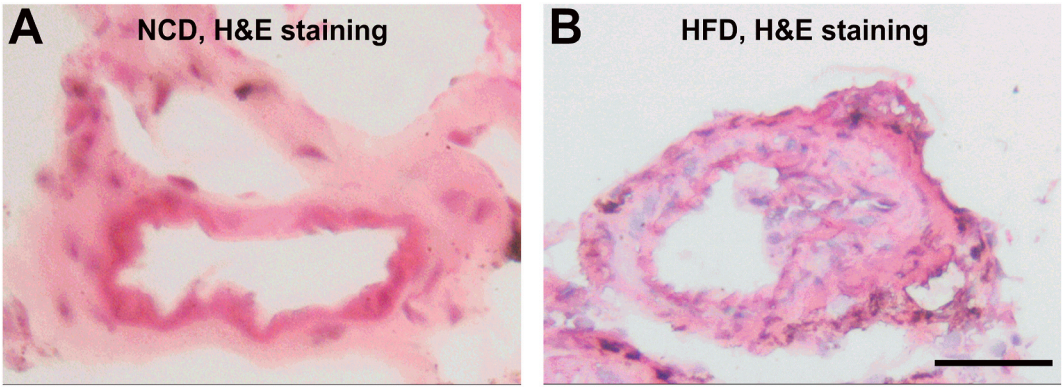

Fig. 6. Ophthalmic artery cross-sections (H&E stain) of mice subjected to normal chow diet (NCD, A) and to high fat diet (HFD, B). Remarkable derangement of the arterial wall architecture was seen in ophthalmic arteries from mice on HFD with marked thickening of the vascular wall at some locations (B). Scale bar = 50 μm.

Remarkably, NOX2 expression was significantly increased in the vascular wall of mice exposed to HFD (Fig. 4C).

3.5. LOX-1 and RAGE expression in the ophthalmic artery

Immunoreactivity to LOX-1 was barely visible in ophthalmic arteries from both mice subjected to HFD and to NCD (Fig. 5A). There was no difference in fluorescent intensity between both groups (Fig. 5B), suggesting that the type of diet has not influence on LOX-1 expression. While immunoreactivity to RAGE was low in the ophthalmic artery from mice subjected to NCD, it was abundant in the ophthalmic artery from mice exposed to HFD (Fig. 5C). Fluorescent intensity was significantly higher in the HFD group compared to the NCD group (Fig. 5D).

3.6. Histological findings

Examination of ophthalmic artery cross-sections stained with H&E revealed remarkable derangement of the vascular wall archictercure in mice on HFD. The arterial wall of mice subjected to a HFD was characterized by an irregular thickness with significant wall hypertrophy at some localizations resulting in a markedly smaller lumen at these sites (Fig. 6).

4. Discussion

Several major new findings emerge from our study. First, ophthalmic arteries from mice subjected to HFD displayed impaired responses to the endothelium-dependent vasodilator, acetylcholine, while responses to

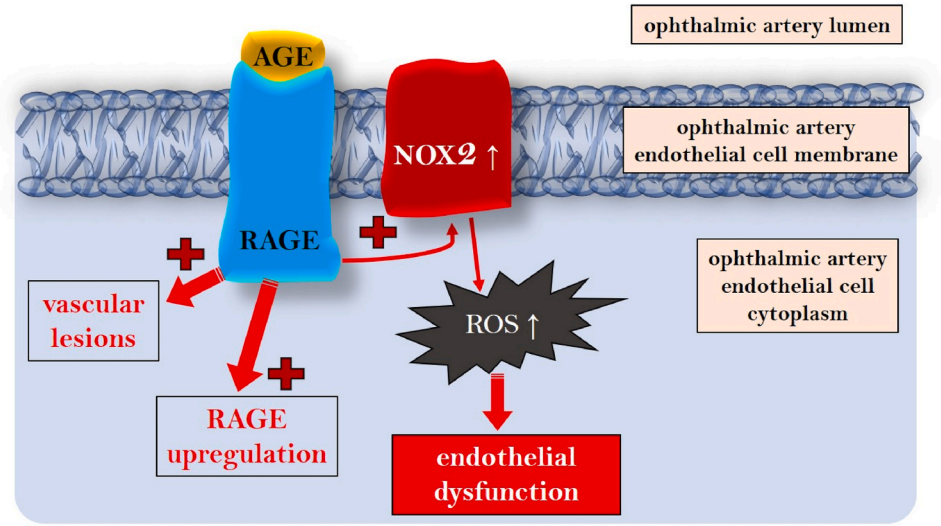

Fig. 7. Possible signaling cascades activated by RAGE in the mouse ophthalmic artery endothelium following exposure to a high-fat diet (HFD), which finally leads to endothelial dysfunction. AGE: advanced glycation endproducts; RAGE: receptor for advanced glycation endproducts; NOX2: nicotinamide adenine dinucleotide phosphate oxidase 2; ROS: reactive oxygen species.

the endothelium-independent vasodilator, SNP, were retained. Thus, ophthalmic artery endothelium presents dysfunction in mice subjected to HFD. Second, ROS levels were elevated in the vascular wall of ophthalmic arteries from mice on HFD. Third, NOX2 levels were raised on both the mRNA and the protein level in ophthalmic arteries from mice exposed to HFD, suggesting that NOX2 is involved in generation of oxidative stress. Furthermore, immunostainings for RAGE and LOX-1 revealed abundant expression of RAGE in ophthalmic arteries from mice exposed to HFD, whereas expression of LOX-1 was low in both mice exposed to HFD and to NCD. These findings speak in favor of an involvement of RAGE, NOX2 and ROS in HFD-induced endothelial dysfunction of the mouse ophthalmic artery rather than the LOX-1 pathway.

Although HFD has previously been reported to induce endothelial dysfunction in blood vessels of various vascular beds and sizes (Clarkson-Townsend et al., 2021; Freeman et al., 2014; Freeman and Granholm, 2012), the current study is the first to describe the effect of HFD on vascular function in the ophthalmic artery, which supplies the eye and other orbital structures with blood. HFD induces obesity together with hypercholesterolemia and hyperglycemia. During hypercholesterolemia, oxidized low-density lipoproteins (Ox-LDLs) trigger the expression of prooxidant enzymes in the vascular wall that contribute to generation of ROS, which at high concentrations, elicit endothelial dysfunction in part by affecting eNOS function and by inactivation of nitric oxide (Alp et al., 2004; Kattoor et al., 2019; Mehta et al., 2007; Simionescu, 2007). Remarkably, LOX-1, which serves as a receptor for ox-LDL, was reported to play a crucial role in this process (Kattoor et al., 2019). The expression of LOX-1 was reported to be upregulated in hypercholesterolemia via positive feedback mechanisms involving the transcription factor, nuclear factor kappa-light-chain-enhancer of activated B cells (NF-κB) (Aoyama et al., 1999; Pérez et al., 2019). In support of this concept, we previously observed endothelial dysfunction as well as elevated LOX-1, NOX2 and ROS levels in retinal arterioles of hypercholesterolemic mice devoid of the apolipoprotein E gene ($ApoE^{-/-}$) (Zadeh et al., 2019b). Surprisingly, we did not find any functional or morphological changes in the ophthalmic artery of $ApoE^{-/-}$ mice in a recent study, although profound endothelial dysfunction, lipid infiltration, ROS accumulation, and elevated NOX and LOX-1 expression was observed in the aorta (Buonfiglio et al., 2023). In obesity, however, hyperglycemia is another factor that may contribute to endothelial dysfunction through oxidative stress, inflammatory processes, glycocalyx damage, cell senescence, and osmotic effects (Dauth et al., 2023; Eshaq et al., 2017; Gericke et al., 2021; Tarr et al., 2013). A crucial role for mediating ROS formation, inflammation and endothelial dysfunction in the vascular wall during hyperglycemia is the pattern recognition receptor, receptor for advanced glycation endproducts (RAGE). Intriguingly, expression of the receptor and of its proinflammatory endogenous ligands is upregulated during states of hyperglycemia in various cell systems via involvement of ROS and NF-κB leading to a vicious cycle of chronic tissue injury and suppression of repair mechanisms (Yan et al., 2009; Yao and Brownlee, 2010).

Our findings suggest that in mice subjected to HFD, LOX-1 was not upregulated in the ophthalmic artery, which is in contrast to our previous study in retinal arterioles of $ApoE^{-/-}$ mice (Zadeh et al., 2019b). Of note, both mouse models develop hypercholesterolemia, a trigger factor for upregulation of LOX-1 expression (Aoyama et al., 1999; Pérez et al., 2019). A possible explanation for this difference may be the different susceptibility of retinal and retrobulbar vessels to hypercholesterolemia, e.g., due to differences in their LOX-1 expression and/or signaling mechanisms. This hypothesis is supported by the observation that human retinal blood vessels displayed reduced vasodilation responses at high cholesterol levels (Reimann et al., 2009; Sharifizad et al., 2016), whereas retrobulbar blood flow velocities did not differ between hypercholesterolemic and control subjects (Senn et al., 1999). In fact, there are various anatomical and functional differences between retrobulbar and retinal blood vessels, e.g., innervation by autonomic nerve fibers, autoregulation as well as endothelium-dependent vasodilation and compensation mechanisms (Delaey and Van De Voorde, 2000; Gericke et al., 2019b, 2013; Manicam et al., 2017, 2016; Németh et al., 2002).

As opposed to LOX-1, RAGE expression was upregulated in the ophthalmic artery from mice exposed to HFD. This is in line with findings of some other studies, in which mice fed a HFD displayed increased RAGE expression in various tissues including blood vessels (Son et al., 2020; Wu et al., 2010). Likewise, murine aortic valves displayed an upregulation of RAGE as well as of its ligands in mice fed a HFD (Hofmann et al., 2014). In the brain of mice subjected to a HFD, an increase of the RAGE ligand S100A8 and upregulation of RAGE has been reported (Loera-Valencia et al., 2021). In Alzheimer's disease, HFD was reported to enhance amyloid β production, a process linked with an increase of RAGE expression in the brain, where this receptor provides the transport of amyloid β from blood to nervous tissues (Ismail et al., 2017).

Remarkably, an investigation examined the retinal expression of proinflammatory and proangiogenic mediators in neonatal diabetic rats fed

a HFD, in diabetic rats fed a NCD and in a non-diabetic control group, showing a significant upregulation of RAGE, TNF-α, ands VEGF in diabetic rats on HFD compared to the other groups (Mancini et al., 2013). Our data provide evidence that HFD in mice produces not only hypercholesterolemia, but also hyperglycemia. Diverse publications reported the association between a diabetic status and an enhanced expression of RAGE. For example, a study on human aortic endothelial cells incubated with high glucose showed that hyperglycemia induced ROS formation and triggered an overexpression of RAGE and its ligands (Yao and Brownlee, 2010). A postmortem investigation assessed an increased expression of RAGE and its ligands in coronary atherosclerotic plaques of diabetic subjects, further associated with apoptosis in macrophages and smooth muscle cells (Burke et al., 2004). Furthermore, a study in diabetic mice demonstrated that RAGE-upregulation is linked with the establishment of vascular lesions as well as with the progression of endothelial injury (Bucciarelli et al., 2002).

The interaction between RAGE and its ligands triggers the upregulation of the receptor (Sorci et al., 2013). Numerous RAGE-ligands were extensively discussed in dedicated studies upon vascular tissues, immune cells or atherosclerotic plaques (Farmer and Kennedy, 2009a), and comprise among others Advanced Glycation End Products (AGEs) (Touré et al., 2008), S100 Calcium-Binding Protein (S100) (Heizmann et al., 2007), high mobility group box 1 protein (Li et al., 2006), macrophage-1 antigen (Orlova et al., 2007), and also oxLDLs (Sun et al., 2009). AGEs are extensively generated under hyperglycemic conditions and play a critical role in ROS generation, leading to vascular impairment (Gao et al., 2008) In monocytes and endothelial cells, activation of RAGE was reported to activate several intracellular cascades, which include c-Jun N-terminal Kinase (JNK), p21-ras MAPK-signaling, phosphatidylinositol-3 kinase (PI–3K)-transduction, with subsequent induction of the extracellular signal-regulated kinase 1 and 2 (ERK1/2) and the Ki-Ras-pathway, culminating in activation of NF-kB (Bartling et al., 2006; D and Jm, 2003; Dukic-Stefanovic et al., 2003; Huttunen et al., 1999; Lander et al., 1997; Vincent et al., 2007). NF-kB is a pivotal actor in the development of inflammation via involvement of interleukin-1 (IL-1), interleukin-6 (IL-6) and tumor necrosis factor-alpha (TNF-α) (Liu et al., 2017), and of angiogenesis, regulating expression of hypoxia-inducible factor 1-alpha (HIF-1α) and vascular endothelial growth factor (VEGF) (Garvey et al., 2009; Romanque et al., 2008). In addition, activated RAGE also induces protein kinase C (PKC), p38 mitogen-activated protein kinase (MAPK) and transforming growth factor-beta (TGF-β) signaling, favoring an increased synthesis of bone matrix proteins, guiding to vascular lesions (Kay et al., 2016a). Moreover, interaction between RAGE and its ligands was shown to promote ROS generation and inflammation via involvement of NOX and NF-kB (Kay et al., 2016b; Wautier et al., 2001). NOX is a main generator of superoxide in the vascular wall, thus being crucial in the production of ROS through the RAGE pathway (Bierhaus et al., 2005; Griendling and Ushio-Fukai, 1997; Wautier et al., 2001). NOX2-generated ROS in bone marrow-derived cells and resident retinal cells were shown to significantly contribute to retinal vascular damage in the diabetic retina (Rojas et al., 2013). Moreover, upregulation of NOX2 and endothelial dysfunction were observed in retinal arterioles following intraocular pressure elevation, ischemia, lipopolysaccharide exposure and hypercholesterolemia (Gericke et al., 2019a; Rojas et al., 2013; Wang et al., 2022; Zadeh et al., 2019a, 2019b). Under conditions of oxidative stress, peroxynitrite, a potent reactive nitrogen species, oxidizes tetrahydrobiopterin, a fundamental cofactor of endothelial nitric oxide synthase (eNOS), thereby "uncoupling" eNOS and reducing the production of nitric oxide, an essential molecule required for proper endothelial function (Farmer and Kennedy, 2009b; Förstermann, 2006). The final result of these events is endothelial dysfunction, resulting in impaired vasorelaxation (Harja et al., 2008). In a previous study, we induced endothelial dysfunction in the mouse ophthalmic artery by exposure to angiotensin II (Birk et al., 2021). This effect was mediated by the angiotensin II type 1 receptor and by NOX2-mediated ROS formation. Remarkably, the NOS and 12/15-lipoxygenase (12/15-LOX) pathways became dysfunctional in angiotensin II-exposed arteries, while partial compensation by the cytochrome P450 oxygenase pathway was observed, suggesting that ROS produced complex changes of endothelial vasodilatory mechanisms in the ophthalmic artery (Birk et al., 2021).

It has been reported that endothelial dysfunction induced by HFD was prevented by exercise, which induced anti-inflammatory effects (Fukao et al., 2010). In this context, NF-κB is a crucial mediator of inflammation (Bierhaus et al., 2006; DiDonato et al., 2012; Lawrence, 2009). RAGE was reported to induce expression of NF-κB, and consequently peripheral inflammation, in mice subjected to a HFD (Song et al., 2014). RAGE is ubiquitously expressed in various retinal cells and plays a central role in microvascular damage under hyperglycemic conditions (Zong et al., 2011). RAGE activation induces ROS production and activates diverse intracellular pathways such as phosphatidylinositol 3-kinase/protein kinase B (PI3K/Akt), Mitogen-Activated Protein Kinase/Extracellular Signal-Regulated Kinase (MAPK/ERK), and NF-κB, subsequently causing mitochondrial damage, endothelial dysfunction, and arteriosclerosis (Madsen-Bouterse et al., 2010).

According to our findings, we propose the following scheme, demonstrating how endothelial signaling mechanisms might be affected by HFD in the mouse ophthalmic artery (Fig. 6).

5. Conclusion

In conclusion, our findings provide evidence that HFD induces hypercholesterolemia and hyperglycemia in mice and triggers endothelial dysfunction in the ophthalmic artery. The mechanism of action seems to involve upregulation of RAGE, but not LOX-1, and of the prooxidant enzyme, NOX2, which appears to trigger ROS generation and endothelial dysfunction. From a clinical point of view, blockade of the RAGE pathway might become useful to treat cardiovascular side effects of obesity.

Author contributions

Conceptualization, A.G., N.X. and H.L.; methodology, A.G., S.J., D. O., N.X., E.W.B., F.B.; software, A.G. and N.X.; validation, A.G. and Q.T.; formal analysis, A.G., N.X., S.J.; investigation, A.G., Q.T., S.J.; resources, A.G., H.L. and N.X.; data curation, A.G. and N.X.; writing—original draft preparation, S.J.; writing—review and editing, A.G., E.W.B., F.B., H.L. and N.P.; visualization, A.G., S.J. and F.B.; supervision, A.G.; project administration, A.G. and S.J.; funding acquisition, A.G., N.X. and N.P. All authors have read and agreed to the published version of the manuscript.

Funding

This research received no external funding.

Institutional review board statement

The animal study protocol was approved by the responsible regulatory authority (Landesuntersuchungsamt Rheinland-Pfalz) (approval number: 23 177-07/G 17-1-020).

Informed consent statement

Not applicable.

Appendice C.

Declaration of competing interest

The authors declare no conflict of interest. The funders had no role in the design of the study; in the collection, analyses, or interpretation of data; in the writing of the manuscript or in the decision to publish the results.

Data availability

Data will be made available on request.

Acknowledgments

We thank Gisela Reifenberg, Department of Pharmacology, University Medical Center, Johannes Gutenberg University Mainz, for her technical assistance with PCR. A part of the work described herein was carried out by S.J. as part of his doctoral thesis.

Appendice A.

Abbreviations	
12/15-LOX	12/15-lipoxygenase
AGEs	advanced Glycation End Products
ApoE$^{-/-}$	apolipoprotein E gene knockout
DHE	dihydroethidium
eNOS	endothelial nitric oxide synthase
ERK	extracellular signal-regulated kinase
HGMB-1	high mobility group box 1 protein
HFD	high-fat diet
HIF-1α	hypoxia-inducible factor-1alpha
IL	interleukin
JNK	c-Jun N-terminal kinase
LOX-1	lectin-like oxidized low-density lipoprotein receptor-1
MAPK	mitogen-activated protein kinase
NCD	normal chow diet
NF-κB	nuclear factor kappa-light-chain-enhancer of activated B cells
NOX	nicotinamide adenine dinucleotide phosphate oxidase
OA	ophthalmic artery
OxLDLs	oxidized low-density lipoproteins
PBS	phosphate-buffered solution
PI-3K	phosphatidylinositol-3 kinase
PKC	protein kinase C
RAGE	receptor for advanced glycation end products
ROS	reactive oxygen species
S100	S100 calcium-binding protein
TNF-α	tumor necrosis factor-alpha
TGF-β	transforming growth factor-beta
VEGF	vascular endothelial growth factor
XDH	xanthine dehydrogenase
XO	xanthine oxidase

Appendice B.

Table 1
Primer sequences used for quantitative PCR analysis.

Gene	Accession Number	Forward	Reverse
NOX1	NM_172203.1	GGAGGAATTAGGCAAAATGGATT	GCTGCATGACCAGCAATGTT
NOX2	NM_007807.2	CCAACTGGGATAACGAGTTCA	GAGAGTTTCAGCCAAGGCTTC
NOX4	NM_015760.2	GGCTGGCCAACGAAGGGGTTAA	GAGGCTGCAGTTGAGGTTCAGGACA
XDH	NM_011723.3	CAGCATCCCCATTGAGTTCA	GCATAGATGGCCCTCTTGTTG
TBP	NM_013684	CTTCGTGCAAGAAATGCTGAAT	CAGTTGTCCGTGGCTCTCTTATT

Table 2
Specifications of antibodies used for immunofluorescence analysis.

Antibody	Article number, company	Species, clonality	Dilution
NOX2	ab129068, Abcam, Waltham, MA, USA	Rabbit, monoclonal	1 : 200
RAGE	ab37647, Abcam, Waltham, MA, USA	Rabbit, polyclonal	1 : 200
LOX-1	bs-2044R, Biozol Diagnostica Vertrieb GmbH, Eching, Germany	Rabbit, polyclonal	1 : 200
RhodamineRed-X-coupled secondary antibody	111-095-003, dianova GmbH, Hamburg, Germany	Goat anti-rabbit, polyclonal	1 : 200

References

Allende-Vigo, M.Z., 2010. Pathophysiologic mechanisms linking adipose tissue and cardiometabolic risk. Endocr. Pract. 16, 692–698. https://doi.org/10.4158/EP09340.RA.

Alp, N.J., McAteer, M.A., Khoo, J., Choudhury, R.P., Channon, K.M., 2004. Increased endothelial tetrahydrobiopterin synthesis by targeted transgenic GTP-cyclohydrolase I overexpression reduces endothelial dysfunction and atherosclerosis in ApoE-knockout mice. Arterioscler. Thromb. Vasc. Biol. 24, 445–450. https://doi.org/10.1161/01.ATV.0000115637.48689.77.

Aoyama, T., Sawamura, T., Furutani, Y., Matsuoka, R., Yoshida, M.C., Fujiwara, H., Masaki, T., 1999. Structure and chromosomal assignment of the human lectin-like oxidized low-density-lipoprotein receptor-1 (LOX-1) gene. Biochem. J. 339 (Pt 1), 177–184.

Apovian, C.M., 2016. Obesity: definition, comorbidities, causes, and burden. Am. J. Manag. Care 22, s176–s185.

Bartling, B., Demling, N., Silber, R.-E., Simm, A., 2006. Proliferative stimulus of lung fibroblasts on lung cancer cells is impaired by the receptor for advanced glycation end-products. Am. J. Respir. Cell Mol. Biol. 34, 83–91. https://doi.org/10.1165/rcmb.2005-0194OC.

Bierhaus, A., Humpert, P.M., Morcos, M., Wendt, T., Chavakis, T., Arnold, B., Stern, D. M., Nawroth, P.P., 2005. Understanding RAGE, the receptor for advanced glycation end products. J. Mol. Med. (Berl.) 83, 876–886. https://doi.org/10.1007/s00109-005-0688-7.

Bierhaus, A., Stern, D.M., Nawroth, P.P., 2006. RAGE in inflammation: a new therapeutic target. Curr. Opin. Invest. Drugs 7, 985–991.

Birk, M., Baum, E., Zadeh, J.K., Manicam, C., Pfeiffer, N., Patzak, A., Helmstädter, J., Steven, S., Kuntic, M., Daiber, A., Gericke, A., 2021. Angiotensin II induces oxidative stress and endothelial dysfunction in mouse ophthalmic arteries via involvement of AT1 receptors and NOX2. Antioxidants 10, 1238. https://doi.org/10.3390/antiox10081238.

Bray, G.A., 2004. Medical consequences of obesity. J. Clin. Endocrinol. Metab. 89, 2583–2589. https://doi.org/10.1210/jc.2004-0535.

Bucciarelli, L.G., Wendt, T., Qu, W., Lu, Y., Lalla, E., Rong, L.L., Goova, M.T., Moser, B., Kislinger, T., Lee, D.C., Kashyap, Y., Stern, D.M., Schmidt, A.M., 2002. RAGE blockade stabilizes established atherosclerosis in diabetic apolipoprotein E-null mice. Circulation 106, 2827–2835. https://doi.org/10.1161/01.cir.0000039325.03698.36.

Buonfiglio, F., Xia, N., Yüksel, C., Manicam, C., Jiang, S., Zadeh, J.K., Musayeva, A., Elksne, E., Pfeiffer, N., Patzak, A., Li, H., Gericke, A., 2023. Studies on the effects of hypercholesterolemia on mouse ophthalmic artery reactivity. Diseases 11, 124. https://doi.org/10.3390/diseases11040124.

Burke, A.P., Kolodgie, F.D., Zieske, A., Fowler, D.R., Weber, D.K., Varghese, P.J., Farb, A., Virmani, R., 2004. Morphologic findings of coronary atherosclerotic plaques in diabetics: a postmortem study. Arterioscler. Thromb. Vasc. Biol. 24, 1266–1271. https://doi.org/10.1161/01.ATV.0000131783.74034.97.

Chang, R.C.-A., Shi, L., Huang, C.C.-Y., Kim, A.J., Ko, M.L., Zhou, B., Ko, G.Y.-P., 2015. High-fat diet-induced retinal dysfunction. Invest. Ophthalmol. Vis. Sci. 56, 2367–2380. https://doi.org/10.1167/iovs.14-16143.

Chronopoulos, P., Manicam, C., Zadeh, J.K., Laspas, P., Unkrig, J.C., Göbel, M.L., Musayeva, A., Pfeiffer, N., Oelze, M., Daiber, A., Li, H., Xia, N., Gericke, A., 2023. Effects of resveratrol on vascular function in retinal ischemia-reperfusion injury. Antioxidants 12, 853. https://doi.org/10.3390/antiox12040853.

Clarkson-Townsend, D.A., Douglass, A.J., Singh, A., Allen, R.S., Uwaifo, I.N., Pardue, M. T., 2021. Impacts of high fat diet on ocular outcomes in rodent models of visual disease. Exp. Eye Res. 204, 108440 https://doi.org/10.1016/j.exer.2021.108440.

D, X., Jm, K., 2003. Phosphatidylinositol 3'-kinase-dependent activation of renal mesangial cell Ki-Ras and ERK by advanced glycation end products. J. Biol. Chem. 278 https://doi.org/10.1074/jbc.M302771200.

Dauth, A., Bręborowicz, A., Ruan, Y., Tang, Q., Zadeh, J.K., Böhm, E.W., Pfeiffer, N., Khedkar, P.H., Patzak, A., Vujacic-Mirski, K., Daiber, A., Gericke, A., 2023. Sulodexide prevents hyperglycemia-induced endothelial dysfunction and oxidative stress in porcine retinal arterioles. Antioxidants 12, 388. https://doi.org/10.3390/antiox12020388.

Delaey, C., Van De Voorde, J., 2000. Regulatory mechanisms in the retinal and choroidal circulation. Ophthalmic Res. 32, 249–256. https://doi.org/10.1159/000055622.

DiDonato, J.A., Mercurio, F., Karin, M., 2012. NF-κB and the link between inflammation and cancer. Immunol. Rev. 246, 379–400. https://doi.org/10.1111/j.1600-065X.2012.01099.x.

Dukic-Stefanovic, S., Gasic-Milenkovic, J., Deuther-Conrad, W., Münch, G., 2003. Signal transduction pathways in mouse microglia N-11 cells activated by advanced glycation endproducts (AGEs). J. Neurochem. 87, 44–55. https://doi.org/10.1046/j.1471-4159.2003.01988.x.

Eshaq, R.S., Aldalati, A.M.Z., Alexander, J.S., Harris, N.R., 2017. Diabetic retinopathy: breaking the barrier. Pathophysiology 24, 229–241. https://doi.org/10.1016/j.pathophys.2017.07.001.

Farmer, D.G.S., Kennedy, S., 2009a. RAGE, vascular tone and vascular disease. Pharmacol. Ther. 124, 185–194. https://doi.org/10.1016/j.pharmthera.2009.06.013.

Farmer, D.G.S., Kennedy, S., 2009b. RAGE, vascular tone and vascular disease. Pharmacol. Ther. 124, 185–194. https://doi.org/10.1016/j.pharmthera.2009.06.013.

Förstermann, U., 2006. Janus-faced role of endothelial NO synthase in vascular disease: uncoupling of oxygen reduction from NO synthesis and its pharmacological reversal. Biol. Chem. 387, 1521–1533. https://doi.org/10.1515/BC.2006.190.

Freeman, L.R., Granholm, A.-C.E., 2012. Vascular changes in rat hippocampus following a high saturated fat and cholesterol diet. J. Cerebr. Blood Flow Metabol. 32, 643–653. https://doi.org/10.1038/jcbfm.2011.168.

Freeman, L.R., Haley-Zitlin, V., Rosenberger, D.S., Granholm, A.-C., 2014. Damaging effects of a high-fat diet to the brain and cognition: a review of proposed mechanisms. Nutr. Neurosci. 17, 241–251. https://doi.org/10.1179/1476830513Y.0000000092.

Fukao, K., Shimada, K., Naito, H., Sumiyoshi, K., Inoue, N., Iesaki, T., Kume, A., Kiyanagi, T., Hiki, M., Hirose, K., Matsumori, R., Ohsaka, H., Takahashi, Y., Toyoda, S., Itoh, S., Miyazaki, T., Tada, N., Daida, H., 2010. Voluntary exercise ameliorates the progression of atherosclerotic lesion formation via anti-inflammatory effects in apolipoprotein E-deficient mice. J. Atherosclerosis Thromb. 17, 1226–1236. https://doi.org/10.5551/jat.4788.

Gao, X., Zhang, H., Schmidt, A.M., Zhang, C., 2008. AGE/RAGE produces endothelial dysfunction in coronary arterioles in type 2 diabetic mice. Am. J. Physiol. Heart Circ. Physiol. 295, H491–H498. https://doi.org/10.1152/ajpheart.00464.2008.

Garvey, J.F., Taylor, C.T., McNicholas, W.T., 2009. Cardiovascular disease in obstructive sleep apnoea syndrome: the role of intermittent hypoxia and inflammation. Eur. Respir. J. 33, 1195–1205. https://doi.org/10.1183/09031936.00111208.

Gericke, A., Goloborodko, E., Sniatecki, J.J., Steege, A., Wojnowski, L., Pfeiffer, N., 2013. Contribution of nitric oxide synthase isoforms to cholinergic vasodilation in murine retinal arterioles. Exp. Eye Res. 109, 60–66. https://doi.org/10.1016/j.exer.2013.01.012.

Gericke, A., Kordasz, M.L., Steege, A., Sanbe, A., Goloborodko, E., Vetter, J.M., Patzak, A., Pfeiffer, N., 2011. Functional role of α1-adrenoceptor subtypes in murine ophthalmic arteries. Invest. Ophthalmol. Vis. Sci. 52, 4795–4799. https://doi.org/10.1167/iovs.11-7516.

Gericke, A., Mann, C., Zadeh, J.K., Musayeva, A., Wolff, I., Wang, M., Pfeiffer, N., Daiber, A., Li, H., Xia, N., Prokosch, V., 2019a. Elevated intraocular pressure causes abnormal reactivity of mouse retinal arterioles. Oxid. Med. Cell. Longev. 2019, 9736047 https://doi.org/10.1155/2019/9736047.

Gericke, A., Mayer, V.G.A., Steege, A., Patzak, A., Neumann, U., Grus, F.H., Joachim, S. C., Choritz, L., Wess, J., Pfeiffer, N., 2009. Cholinergic responses of ophthalmic arteries in M3 and M5 muscarinic acetylcholine receptor knockout mice. Invest. Ophthalmol. Vis. Sci. 50, 4822–4827. https://doi.org/10.1167/iovs.09-3600.

Gericke, A., Steege, A., Manicam, C., Böhmer, T., Wess, J., Pfeiffer, N., 2014. Role of the M3 muscarinic acetylcholine receptor subtype in murine ophthalmic arteries after endothelial removal. Invest. Ophthalmol. Vis. Sci. 55, 625–631. https://doi.org/10.1167/iovs.13-13549.

Gericke, A., Suminska-Jasińska, K., Bręborowicz, A., 2021. Sulodexide reduces glucose induced senescence in human retinal endothelial cells. Sci. Rep. 11, 11532 https://doi.org/10.1038/s41598-021-90987-w.

Gericke, A., Wolff, I., Musayeva, A., Zadeh, J.K., Manicam, C., Pfeiffer, N., Li, H., Xia, N., 2019b. Retinal arteriole reactivity in mice lacking the endothelial nitric oxide synthase (eNOS) gene. Exp. Eye Res. 181, 150–156. https://doi.org/10.1016/j.exer.2019.01.022.

Griendling, K.K., Ushio-Fukai, M., 1997. NADH/NADPH oxidase and vascular function. Trends Cardiovasc. Med. 7, 301–307. https://doi.org/10.1016/S1050-1738(97)00088-1.

Harja, E., Bu, D., Hudson, B.I., Chang, J.S., Shen, X., Hallam, K., Kalea, A.Z., Lu, Y., Rosario, R.H., Oruganti, S., Nikolla, Z., Belov, D., Lalla, E., Ramasamy, R., Yan, S.F., Schmidt, A.M., 2008. Vascular and inflammatory stresses mediate atherosclerosis via RAGE and its ligands in apoE-/- mice. J. Clin. Invest. 118, 183–194. https://doi.org/10.1172/JCI32703.

Health, I. of M. (US) C. on D., Woteki, C.E., Thomas, P.R., 1992. Fats, Cholesterol, and Chronic Diseases, Eat for Life: the Food and Nutrition Board's Guide to Reducing Your Risk of Chronic Disease. National Academies Press (US).

Heizmann, C.W., Ackermann, G.E., Galichet, A., 2007. Pathologies involving the S100 proteins and RAGE. Subcell. Biochem. 45, 93–138. https://doi.org/10.1007/978-1-4020-6191-2_5.

Hofmann, B., Yakobus, Y., Indrasari, M., Nass, N., Santos, A.N., Kraus, F.B., Silber, R.-E., Simm, A., 2014. RAGE influences the development of aortic valve stenosis in mice on a high fat diet. Exp. Gerontol. 59, 13–20. https://doi.org/10.1016/j.exger.2014.05.001.

Huttunen, H.J., Fages, C., Rauvala, H., 1999. Receptor for advanced glycation end products (RAGE)-mediated neurite outgrowth and activation of NF-kappaB require the cytoplasmic domain of the receptor but different downstream signaling pathways. J. Biol. Chem. 274, 19919–19924. https://doi.org/10.1074/jbc.274.28.19919.

Ismail, N., Ismail, M., Azmi, N.H., Bakar, M.F.A., Yida, Z., Abdullah, M.A., Basri, H., 2017. Thymoquinone-rich fraction nanoemulsion (TQRFNE) decreases Aβ40 and Aβ42 levels by modulating APP processing, up-regulating IDE and LRP1, and down-regulating BACE1 and RAGE in response to high fat/cholesterol diet-induced rats. Biomed. Pharmacother. 95, 780–788. https://doi.org/10.1016/j.biopha.2017.08.074.

Kattoor, A.J., Kanuri, S.H., Mehta, J.L., 2019. Role of ox-LDL and LOX-1 in atherogenesis. Curr. Med. Chem. 26, 1693–1700. https://doi.org/10.2174/0929867325666180508100950.

Kay, A.M., Simpson, C.L., Stewart, J.A., 2016a. The role of AGE/RAGE signaling in diabetes-mediated vascular calcification. J. Diabetes Res. 2016, 6809703 https://doi.org/10.1155/2016/6809703.

Kay, A.M., Simpson, C.L., Stewart, J.A., 2016b. The role of AGE/RAGE signaling in diabetes-mediated vascular calcification. J. Diabetes Res. 2016, 6809703 https://doi.org/10.1155/2016/6809703.

Kopec, A.K., Abrahams, S.R., Thornton, S., Palumbo, J.S., Mullins, E.S., Divanovic, S., Weiler, H., Owens, A.P., Mackman, N., Goss, A., van Ryn, J., Luyendyk, J.P.,

Flick, M.J., 2017. Thrombin promotes diet-induced obesity through fibrin-driven inflammation. J. Clin. Invest. 127, 3152–3166. https://doi.org/10.1172/JCI92744.
Lander, H.M., Tauras, J.M., Ogiste, J.S., Hori, O., Moss, R.A., Schmidt, A.M., 1997. Activation of the receptor for advanced glycation end products triggers a p21(ras)-dependent mitogen-activated protein kinase pathway regulated by oxidant stress. J. Biol. Chem. 272, 17810–17814. https://doi.org/10.1074/jbc.272.28.17810.
Lawrence, T., 2009. The nuclear factor NF-kappaB pathway in inflammation. Cold Spring Harbor Perspect. Biol. 1, a001651. https://doi.org/10.1101/cshperspect.a001651.
Li, J., Wu, H., Liu, Y., Yang, L., 2020. High fat diet induced obesity model using four strainsof mice: kunming, C57BL/6, BALB/c and ICR. Exp. Anim. 69, 326–335. https://doi.org/10.1538/expanim.19-0148.
Li, W., Sama, A.E., Wang, H., 2006. Role of HMGB1 in cardiovascular diseases. Curr. Opin. Pharmacol. 6, 130–135. https://doi.org/10.1016/j.coph.2005.10.010.
Liu, T., Zhang, L., Joo, D., Sun, S.-C., 2017. NF-κB signaling in inflammation. Signal Transduct. Targeted Ther. 2, 17023 https://doi.org/10.1038/sigtrans.2017.23.
Loera-Valencia, R., Ismail, M.-A.-M., Goikolea, J., Lodeiro, M., Mateos, L., Björkhem, I., Puerta, E., Romão, M.A., Gomes, C.M., Merino-Serrais, P., Maioli, S., Cedazo-Minguez, A., 2021. Hypercholesterolemia and 27-hydroxycholesterol increase S100A8 and RAGE expression in the brain: a link between cholesterol, alarmins, and neurodegeneration. Mol. Neurobiol. 58, 6063–6076. https://doi.org/10.1007/s12035-021-02521-8.
Madsen-Bouterse, S.A., Mohammad, G., Kanwar, M., Kowluru, R.A., 2010. Role of mitochondrial DNA damage in the development of diabetic retinopathy, and the metabolic memory phenomenon associated with its progression. Antioxidants Redox Signal. 13, 797–805. https://doi.org/10.1089/ars.2009.2932.
Mancini, J.E., Ortiz, G., Croxatto, J.O., Gallo, J.E., 2013. Retinal upregulation of inflammatory and proangiogenic markers in a model of neonatal diabetic rats fed on a high-fat-diet. BMC Ophthalmol. 13, 14. https://doi.org/10.1186/1471-2415-13-14.
Manicam, C., Ginter, N., Li, H., Xia, N., Goloborodko, E., Zadeh, J.K., Musayeva, A., Pfeiffer, N., Gericke, A., 2017. Compensatory vasodilator mechanisms in the ophthalmic artery of endothelial nitric oxide synthase gene knockout mice. Sci. Rep. 7, 7111. https://doi.org/10.1038/s41598-017-07768-7.
Manicam, C., Staubitz, J., Brochhausen, C., Grus, F.H., Pfeiffer, N., Gericke, A., 2016. The gatekeepers in the mouse ophthalmic artery: endothelium-dependent mechanisms of cholinergic vasodilation. Sci. Rep. 6, 20322 https://doi.org/10.1038/srep20322.
Mehta, J.L., Sanada, N., Hu, C.P., Chen, J., Dandapat, A., Sugawara, F., Satoh, H., Inoue, K., Kawase, Y., Jishage, K., Suzuki, H., Takeya, M., Schnackenberg, L., Beger, R., Hermonat, P.L., Thomas, M., Sawamura, T., 2007. Deletion of LOX-1 reduces atherogenesis in LDLR knockout mice fed high cholesterol diet. Circ. Res. 100, 1634–1642. https://doi.org/10.1161/CIRCRESAHA.107.149724.
Mozaffarian, D., Hao, T., Rimm, E.B., Willett, W.C., Hu, F.B., 2011. Changes in diet and lifestyle and long-term weight gain in women and men. N. Engl. J. Med. 364, 2392–2404. https://doi.org/10.1056/NEJMoa1014296.
Nagy, C., Einwallner, E., 2018. Study of in vivo glucose metabolism in high-fat diet-fed mice using oral glucose tolerance test (OGTT) and insulin tolerance test (ITT). J. Vis. Exp. 56672 https://doi.org/10.3791/56672.
Németh, J., Knézy, K., Tapasztó, B., Kovács, R., Harkányi, Z., 2002. Different autoregulation response to dynamic exercise in ophthalmic and central retinal arteries: a color Doppler study in healthy subjects. Graefes Arch. Clin. Exp. Ophthalmol. 240, 835–840. https://doi.org/10.1007/s00417-002-0552-1.
Orlova, V.V., Choi, E.Y., Xie, C., Chavakis, E., Bierhaus, A., Ihanus, E., Ballantyne, C.M., Gahmberg, C.G., Bianchi, M.E., Nawroth, P.P., Chavakis, T., 2007. A novel pathway of HMGB1-mediated inflammatory cell recruitment that requires Mac-1-integrin. EMBO J. 26, 1129–1139. https://doi.org/10.1038/sj.emboj.7601552.
Ouchi, N., Parker, J.L., Lugus, J.J., Walsh, K., 2011. Adipokines in inflammation and metabolic disease. Nat. Rev. Immunol. 11, 85–97. https://doi.org/10.1038/nri2921.
Pérez, L., Vallejos, A., Echeverria, C., Varela, D., Cabello-Verrugio, C., Simon, F., 2019. OxHDL controls LOX-1 expression and plasma membrane localization through a mechanism dependent on NOX/ROS/NF-κB pathway on endothelial cells. Lab. Invest. 99, 421–437. https://doi.org/10.1038/s41374-018-0151-3.
Reimann, M., Prieur, S., Lippold, B., Bornstein, S.R., Reichmann, H., Julius, U., Ziemssen, T., 2009. Retinal vessel analysis in hypercholesterolemic patients before and after LDL apheresis. Atherosclerosis Suppl. 10, 39–43. https://doi.org/10.1016/S1567-5688(09)71808-2.
Rojas, M., Zhang, W., Xu, Z., Lemtalsi, T., Chandler, P., Toque, H.A., Caldwell, R.W., Caldwell, R.B., 2013. Requirement of NOX2 expression in both retina and bone marrow for diabetes-induced retinal vascular injury. PLoS One 8, e84357. https://doi.org/10.1371/journal.pone.0084357.
Romanque, P., Piguet, A.-C., Dufour, J.-F., 2008. Targeting vessels to treat hepatocellular carcinoma. Clin. Sci. (Lond.) 114, 467–477. https://doi.org/10.1042/CS20070310.
Schröder, K., Vecchione, C., Jung, O., Schreiber, J.G., Shiri-Sverdlov, R., van Gorp, P.J., Busse, R., Brandes, R.P., 2006. Xanthine oxidase inhibitor tungsten prevents the development of atherosclerosis in ApoE knockout mice fed a Western-type diet. Free Radic. Biol. Med. 41, 1353–1360. https://doi.org/10.1016/j.freeradbiomed.2006.03.026.
Senn, B., Orgul, S., Keller, U., Dickermann, D., Dubler, B., Vavrecka, J., Gasser, P., Kaiser, H.J., Flammer, J., 1999. Retrobulbar and peripheral capillary blood flow in hypercholesterolemic subjects. Am. J. Ophthalmol. 128, 310–316. https://doi.org/10.1016/s0002-9394(99)00148-8.
Sharifizad, M., Witkowska, K.J., Aschinger, G.C., Sapeta, S., Rauch, A., Schmidl, D., Werkmeister, R.M., Garhöfer, G., Schmetterer, L., 2016. Factors determining flicker-induced retinal vasodilation in healthy subjects. Invest. Ophthalmol. Vis. Sci. 57, 3306–3312. https://doi.org/10.1167/iovs.16-19261.
Simionescu, M., 2007. Implications of early structural-functional changes in the endothelium for vascular disease. Arterioscler. Thromb. Vasc. Biol. 27, 266–274. https://doi.org/10.1161/01.ATV.0000253884.13901.e4.
Son, M., Oh, S., Jang, J.T., Park, C.-H., Son, K.H., Byun, K., 2020. Attenuating effects of pyrogallol-phloroglucinol-6,6-bieckol on vascular smooth muscle cell phenotype changes to osteoblastic cells and vascular calcification induced by high fat diet. Nutrients 12, 2777. https://doi.org/10.3390/nu12092777.
Song, F., Hurtado del Pozo, C., Rosario, R., Zou, Y.S., Ananthakrishnan, R., Xu, X., Patel, P.R., Benoit, V.M., Yan, S.F., Li, H., Friedman, R.A., Kim, J.K., Ramasamy, R., Ferrante Jr., A.W., Schmidt, A.M., 2014. RAGE regulates the metabolic and inflammatory response to high-fat feeding in mice. Diabetes 63, 1948–1965. https://doi.org/10.2337/db13-1636.
Sorci, G., Riuzzi, F., Giambanco, I., Donato, R., 2013. RAGE in tissue homeostasis, repair and regeneration. Biochim. Biophys. Acta 1833, 101–109. https://doi.org/10.1016/j.bbamcr.2012.10.021.
Sun, L., Ishida, T., Yasuda, T., Kojima, Y., Honjo, T., Yamamoto, Y., Yamamoto, H., Ishibashi, S., Hirata, K., Hayashi, Y., 2009. RAGE mediates oxidized LDL-induced pro-inflammatory effects and atherosclerosis in non-diabetic LDL receptor-deficient mice. Cardiovasc. Res. 82, 371–381. https://doi.org/10.1093/cvr/cvp036.
Tarr, J.M., Kaul, K., Chopra, M., Kohner, E.M., Chibber, R., 2013. Pathophysiology of diabetic retinopathy. ISRN Ophthalmol 2013, 343560. https://doi.org/10.1155/2013/343560.
Touré, F., Zahm, J.-M., Garnotel, R., Lambert, E., Bonnet, N., Schmidt, A.M., Vitry, F., Chanard, J., Gillery, P., Rieu, P., 2008. Receptor for advanced glycation end-products (RAGE) modulates neutrophil adhesion and migration on glycoxidated extracellular matrix. Biochem. J. 416, 255–261. https://doi.org/10.1042/BJ20080054.
Vincent, A.M., Perrone, L., Sullivan, K.A., Backus, C., Sastry, A.M., Lastoskie, C., Feldman, E.L., 2007. Receptor for advanced glycation end products activation injures primary sensory neurons via oxidative stress. Endocrinology 148, 548–558. https://doi.org/10.1210/en.2006-0073.
Wang, C.-Y., Liao, J.K., 2012a. A mouse model of diet-induced obesity and insulin resistance. In: Weichhart, T. (Ed.), MTOR: Methods and Protocols, 分子生物学方法. Humana Press, Totowa, NJ, pp. 421–433. https://doi.org/10.1007/978-1-61779-430-8_27.
Wang, C.-Y., Liao, J.K., 2012b. A mouse model of diet-induced obesity and insulin resistance. Methods Mol. Biol. 821, 421–433. https://doi.org/10.1007/978-1-61779-430-8_27.
Wang, M., Liu, H., Xia, N., Li, H., van Beers, T., Gericke, A., Prokosch, V., 2022. Intraocular pressure-induced endothelial dysfunction of retinal blood vessels is persistent, but does not trigger retinal ganglion cell loss. Antioxidants 11, 1864. https://doi.org/10.3390/antiox11101864.
Wautier, M.P., Chappey, O., Corda, S., Stern, D.M., Schmidt, A.M., Wautier, J.L., 2001. Activation of NADPH oxidase by AGE links oxidant stress to altered gene expression via RAGE. Am. J. Physiol. Endocrinol. Metab. 280, E685–E694. https://doi.org/10.1152/ajpendo.2001.280.5.E685.
Wu, J., Zhao, M., Zheng, H., Zhang, H., Jiang, Y., 2010. Pentoxifylline alleviates high-fat diet-induced non-alcoholic steatohepatitis and early atherosclerosis in rats by inhibiting AGE and RAGE expression. Acta Pharmacol. Sin. 31, 1367–1375. https://doi.org/10.1038/aps.2010.110.
Xia, N., Horke, S., Habermeier, A., Closs, E.I., Reifenberg, G., Gericke, A., Mikhed, Y., Münzel, T., Daiber, A., Förstermann, U., Li, H., 2016a. Uncoupling of endothelial nitric oxide synthase in perivascular adipose tissue of diet-induced obese mice. Arterioscler. Thromb. Vasc. Biol. 36, 78–85. https://doi.org/10.1161/ATVBAHA.115.306263.
Xia, N., Horke, S., Habermeier, A., Closs, E.I., Reifenberg, G., Gericke, A., Mikhed, Y., Münzel, T., Daiber, A., Förstermann, U., Li, H., 2016b. Uncoupling of endothelial nitric oxide synthase in perivascular adipose tissue of diet-induced obese mice. Arterioscler. Thromb. Vasc. Biol. 36, 78–85. https://doi.org/10.1161/ATVBAHA.115.306263.
Yan, S.F., Ramasamy, R., Schmidt, A.M., 2009. Receptor for AGE (RAGE) and its ligands-cast into leading roles in diabetes and the inflammatory response. J. Mol. Med. (Berl.) 87, 235–247. https://doi.org/10.1007/s00109-009-0439-2.
Yao, D., Brownlee, M., 2010. Hyperglycemia-induced reactive oxygen species increase expression of the receptor for advanced glycation end products (RAGE) and RAGE ligands. Diabetes 59, 249–255. https://doi.org/10.2337/db09-0801.
Zadeh, J.K., Garcia-Bardon, A., Hartmann, E.K., Pfeiffer, N., Omran, W., Ludwig, M., Patzak, A., Xia, N., Li, H., Gericke, A., 2019a. Short-time ocular ischemia induces vascular endothelial dysfunction and ganglion cell loss in the pig retina. Int. J. Mol. Sci. 20, 4685. https://doi.org/10.3390/ijms20194685.
Zadeh, J.K., Zhutdieva, M.B., Laspas, P., Yuksel, C., Musayeva, A., Pfeiffer, N., Brochhausen, C., Oelze, M., Daiber, A., Xia, N., Li, H., Gericke, A., 2019b. Apolipoprotein E deficiency causes endothelial dysfunction in the mouse retina. Oxid. Med. Cell. Longev. 2019, 5181429 https://doi.org/10.1155/2019/5181429.
Zhang, B., Qiu, Q., Yin, L., Yao, Y., Wang, C., Wu, X., 2014. Measurement of retinal function with flash-electroretinography in Chinese patients with hyperlipidemia. Graefes Arch. Clin. Exp. Ophthalmol. 252, 1385–1392. https://doi.org/10.1007/s00417-014-2726-z.
Zhang, X.Y., Guo, C.C., Yu, Y.X., Xie, L., Chang, C.Q., 2020. [Establishment of high-fat diet-induced obesity and insulin resistance model in rats]. Beijing Da Xue Xue Bao Yi Xue Ban 52, 557–563. https://doi.org/10.19723/j.issn.1671-167X.2020.03.024.
Zong, H., Ward, M., Stitt, A.W., 2011. AGEs, RAGE, and diabetic retinopathy. Curr. Diabetes Rep. 11, 244–252. https://doi.org/10.1007/s11892-011-0198-7.